Asian Research Journal of Mathematics

Volume 22, Issue 8, Page 80-90, 2026; Article no.ARJOM.163418
ISSN: 2456-477X

Hydrodynamic Modelling of Mixing Efficiency and Optimal Bio-methane Production in Anaerobic Digesters Using a Two-Dimensional Navier–Stokes Framework

Ruth Akumu Obande [a*], Joseph Kandie [a] and Albert Bii [a]

[a] Department of Mathematics and Computer Science, University of Eldoret, Eldoret, Kenya.

Authors' contributions

This work was carried out in collaboration among all authors. Author RAO designed the study, performed the mathematical formulation and MATLAB simulations, and wrote the first draft of the manuscript. Authors JK and AB supervised the study, reviewed the model formulation, and revised the manuscript. All authors read and approved the final manuscript.

Article Information

DOI: https://doi.org/10.9734/arjom/2026/v22i81136

Open Peer Review History:
This journal follows the Advanced Open Peer Review policy. Identity of the Reviewers, Editor(s) and additional Reviewers, peer review comments, different versions of the manuscript, comments of the editors, etc are available here: https://pr.sdiarticle5.com/review-history/163418

Original Research Article

Received: 28/05/2026
Accepted: 27/07/2026
Published: 03/08/2026

Abstract

Background: Anaerobic digestion (AD) is a proven technology for renewable bio-methane production, but digester efficiency is often limited by poor hydrodynamic mixing rather than by microbial kinetics alone; most existing models, however, assume idealised, fully homogeneous reactors.
Objective: This study investigates the influence of hydrodynamics on mixing efficiency and bio-methane production potential in anaerobic digesters using mathematical modelling.

**Corresponding author: Email: ruthakumu33@gmail.com;*

Cite as: *Obande, R. A., Kandie, J., & Bii, A. (2026). Hydrodynamic Modelling of Mixing Efficiency and Optimal Bio-methane Production in Anaerobic Digesters Using a Two-Dimensional Navier–Stokes Framework. Asian Research Journal of Mathematics, 22(8), 80–90. https://doi.org/10.9734/arjom/2026/v22i81136*

Methods: A two-dimensional incompressible Navier–Stokes model was coupled with a tracer advection–diffusion equation to simulate slurry flow and mixing behaviour. The governing equations were non-dimensionalised using the Reynolds and Péclet numbers, discretised using the finite difference method, and solved numerically in MATLAB. An optimisation framework that treated inlet velocity as the control variable, together with an adjoint sensitivity analysis, was used to evaluate and improve mixing efficiency.
Results: At a Reynolds number of 2100, the flow exhibited transitional characteristics, with a dead zone fraction of approximately 35.1%. Velocity contours revealed limited circulation, whereas the tracer distribution showed a non-uniform concentration pattern across the domain. The dead zone fraction declined exponentially as Re increased, with values above 4000 projected to reduce it below 15%. At Pe = 10,000, transport was strongly advection-dominated, and the adjoint sensitivity analysis identified the inlet/impeller region as offering the greatest leverage over mixing performance.
Conclusion: Hydrodynamic conditions play a critical role in determining mixing efficiency and, consequently, bio-methane production potential. The developed model provides a computationally efficient framework for analysing and optimising anaerobic digester performance and offers a foundation for future integration with biochemical reaction models.

Keywords: Anaerobic digestion; bio-methane production; hydrodynamic modelling; two-dimensional Navier–Stokes equations; computational fluid dynamics; tracer transport; mixing efficiency; dead zones; Reynolds number; Péclet number; adjoint sensitivity analysis; optimal control.

List of Abbreviations

Abbreviations / Symbol	Meaning
Re	*Reynolds Number*
Pe	*Péclet Number*
∇	*Laplacian operator*
2D	*Two dimension*
C	*Tracer concentration*
F	*External force in y direction*
D	*Diffusion coefficient*
dt	*Time step (s)*
F_x, F_y	*External forces in x and y directions*
P	*Pressure (Pa)*
t	*Time (s)*
ρ	*Fluid density (kg/m³)*
u	*Velocity in x direction (m/s)*
v	*Velocity in y direction (m/s)*
U	*Characteristic velocity (m/s)*
μ	*Dynamic viscosity (Pa·s)*
x, y	*Spatial coordinates (m)*
L	*Characteristic length (m)*
k	*Rate constant*
n	*Flow behavior index*
$\bar{C}$	*Spatial average concentration*
Ω	*Digester domain*
λ	*Adjoint (Lagrange multiplier)*

1 Introduction

Anaerobic digestion (AD) converts organic feedstocks—livestock manure, crop residues, and food waste—into biogas under oxygen-free conditions, yielding a methane-rich fuel alongside a nutrient-rich digestate (Mao et al., 2015). As countries pursue climate-resilient, locally available energy sources, bio-methane from AD offers a continuous, low-cost complement to intermittent renewables such as solar and wind and is particularly attractive in resource-limited settings. Recent studies using agricultural residues and mixed organic feedstocks have further demonstrated the feasibility of biogas production under anaerobic conditions, supporting continued efforts to improve digester performance through better process design (Dibua et al., 2025; Enenebeaku et al., 2026).

Despite this potential, digester performance is routinely constrained by inadequate mixing rather than by microbial kinetics alone. Most published AD models assume idealised, fully homogeneous reactors and focus on substrate consumption and microbial kinetics, while real digesters—particularly low-cost or large-scale units common in low- and middle-income countries—exhibit non-uniform flow, localised stagnant ("dead") zones, solids settling, and uneven mass transfer (Bridgeman, 2012; Craig et al., 2013). These hydrodynamic deficiencies reduce contact between microorganisms and the substrate, thereby slowing digestion and reducing methane output (Kariyama et al., 2018).

Computational fluid dynamics (CFD), grounded in the Navier–Stokes equations, offers a rigorous means of resolving these internal flow patterns. However, much of the existing CFD literature on digesters relies on computationally expensive three-dimensional simulations or focuses on mechanically mixed systems that are uncommon in low-resource installations (Craig et al., 2013; Oates et al., 2020). Recent rheology-informed and coupled hydrodynamic–biokinetic studies further indicate that spatial flow heterogeneity can materially affect model predictions and mixing assessments in anaerobic digesters (Wei et al., 2023; Kumar et al., 2024). Simultaneously, numerical and analytical methodologies for scalar advection–diffusion transport and differential systems—including advanced analytical transformations, conformable derivatives, and homotopy-based techniques—have made substantial progress in clarifying transport phenomena across physical media (Alkan, 2024; Aktürk et al., 2024; Avit & Anaç, 2024). There remains a clear gap in simplified, computationally efficient hydrodynamic models—such as two-dimensional Navier–Stokes formulations—that retain physical fidelity while remaining tractable on standard hardware and explicitly link flow behaviour to a measurable mixing-efficiency metric and bio-methane production potential. Multiscale CFD analysis has also shown that reactor geometry and operating configuration influence mixing uniformity in high-solids digestion systems (Hua et al., 2025). However, the literature reviewed in this manuscript does not yet provide a computationally light, two-dimensional framework that combines tracer-based dead-zone quantification with adjoint sensitivity analysis to identify high-leverage mixing interventions.

This study addresses that gap. We develop a two-dimensional, incompressible Navier–Stokes hydrodynamic model coupled with a scalar tracer transport equation to characterise slurry flow, quantify dead zones, and assess mixing efficiency in an anaerobic digester. The model is embedded within an optimal-control framework in which inlet velocity is treated as the control variable, and an adjoint formulation identifies the regions most sensitive to improvements in mixing. The specific objectives are to:

1. Formulate the 2D Navier–Stokes equations describing slurry flow inside the digester;
2. Quantify mixing efficiency and dead zone formation using tracer-based transport analysis;
3. Determine the operating conditions—through inlet velocity, viscosity, and diffusivity—that optimise mixing performance.

2 Methodology

2.1 Model Framework

Slurry motion within the two-dimensional, incompressible digester domain Ω is governed by the Navier–Stokes equations:

$$\rho(\frac{\partial u}{\partial t} + u\frac{\partial u}{\partial x} + v\frac{\partial u}{\partial y}) = -\frac{\partial p}{\partial x} + \mu\,(\frac{\partial^2 u}{\partial x^2} + \frac{\partial^2 u}{\partial y^2}) + F_x \quad (2.1)$$

$$\rho\left(\frac{\partial v}{\partial t} + u\frac{\partial v}{\partial x} + v\frac{\partial v}{\partial y}\right) = -\frac{\partial p}{\partial y} + \mu(\frac{\partial^2 v}{\partial x^2} + \frac{\partial^2 v}{\partial y^2}) + F_y \quad (2.2)$$

In vector form, Equations (2.1) and (2.2) are written as:

$$\rho(\frac{\partial U}{\partial t} + U \cdot \nabla U) = -\nabla p + \mu\nabla^2 U + F \quad (2.3)$$

Tracer transport used to evaluate mixing is governed by the advection–diffusion equation:

$$\frac{\partial C}{\partial t} = D\left(\frac{\partial^2 C}{\partial x^2} + \frac{\partial^2 C}{\partial y^2}\right) - u\frac{\partial C}{\partial x} - v\frac{\partial C}{\partial y} \tag{2.4}$$

Non-dimensionalising using the characteristic velocity U, length L, and reference concentration C_0 yields:

$$\frac{\partial u^*}{\partial t^*} + (u^*.\nabla^*)u^* = -\nabla^* p^* + \frac{1}{Re}\nabla^{*2}u^* + F^* \tag{2.5}$$

$$\frac{\partial C^*}{\partial t^*} + (u^*.\nabla^*)C^* = \frac{1}{Pe}\nabla^{*2}C^* \tag{2.6}$$

2.2 Assumptions and Approximations

The model rests on four primary assumptions:

- Two-dimensional, incompressible flow.
- A Newtonian fluid assumption. While bio-slurries exhibit non-Newtonian shear-thinning characteristics at high total solids content, the Newtonian assumption provides a computationally tractable, first-order approximation capable of identifying global flow structures and primary recirculation loops in low-cost digesters operating at low-to-moderate solids levels.
- Flow driven by combined inlet jetting and external impeller forcing.
- A non-reactive scalar tracer with constant diffusion coefficient.

2.3 Discretisation Scheme and Numerical Stability

The domain is discretised on a structured grid with uniform spatial steps Δx and Δy. The discretised momentum equations in the x and y directions are:

$$\frac{U_{i,j}^{\ n+1}-U_{i,j}^n}{\Delta t} + U_{i,j}^n\frac{U_{i+1,j}^n-U_{i-1,j}^n}{2\Delta x} + V_{i,j}^n\frac{U_{i,j+1}^n-U_{i,j-1}^n}{2\Delta y} = -\frac{1}{\rho}\frac{P_{i+1,j}^n-P_{i-1,j}^n}{2\Delta x} + \frac{1}{Re}\left(\frac{U_{i+1,j}^n-2U_{i,j}^n+U_{i-1,j}^n}{\Delta x^2} + \frac{U_{i,j+1}^n-2U_{i,j}^n+U_{i,j-1}^n}{\Delta y^2}\right) + \Delta t\,(F_{x,i,j}^{\ n}) \tag{2.7}$$

$$\frac{V_{i,j}^{\ n+1}-V_{i,j}^n}{\Delta t} + U_{i,j}^n\frac{V_{i+1,j}^n-V_{i-1,j}^n}{2\Delta x} + V_{i,j}^n\frac{V_{i,j+1}^n-V_{i,j-1}^n}{2\Delta y} = -\frac{1}{\rho}\frac{P_{i+1,j}^n-P_{i-1,j}^n}{2\Delta y} + \frac{1}{Re}\left(\frac{V_{i+1,j}^n-2V_{i,j}^n+V_{i-1,j}^n}{\Delta x^2} + \frac{V_{i,j+1}^n-2V_{i,j}^n+V_{i,j-1}^n}{\Delta y^2}\right) + \Delta t\,(F_{y,i,j}^n) \tag{2.8}$$

The scalar tracer advection–diffusion discretisation is expressed as:

$$C_{i,j}^{n+1} = C_{i,j}^{\ n} - \Delta t\left(u_{i,j}^n\frac{C_{i+1,j}^n-C_{i-1,j}^n}{2\Delta x} + v_{i,j}^n\frac{C_{i,j+1}^n-C_{i,j-1}^n}{2\Delta y}\right) + \frac{1}{Pe}\Delta t\left(\frac{C_{i+1,j}^n-2C_{i,j}^n+C_{i-1,j}^n}{\Delta x^2} + \frac{C_{i,j+1}^n-2C_{i,j}^n+C_{i,j-1}^n}{\Delta y^2}\right) \tag{2.9}$$

Numerical Stability Note: Although the Forward-Time Central-Space (FTCS) discretisation of the advection terms is conditionally unstable for purely advective flow, stability in this implementation is maintained by enforcing the local cell Péclet and cell Reynolds numbers, $\boldsymbol{Pe_c ell = |u|.\Delta x.Pe \leq 2}$, applying standard upwind blending to the convective terms and using a fine spatial resolution $\boldsymbol{\Delta x = L_x/200}$, $\boldsymbol{\Delta y = L_y/100}$, and imposing strict Courant–Friedrichs–Lewy (CFL) time-step constraints:

$$\Delta t \leq \min\left(\frac{\Delta x}{|u|max}, \frac{\Delta y}{|v|max}, \frac{Re}{2}\left(\frac{1}{\Delta x^2} + \frac{1}{\Delta y^2}\right)^{-1}\right)$$

2.4 Optimal Control and Adjoint Formulation

To minimise non-uniformity, we define the objective functional $J(C)$ as the spatial variance of tracer concentration over the domain Ω:

$$J(C) = \int_{\Omega} \left(C_{(x,y,t)} - \bar{C}\right)^2 dA \tag{2.10}$$

where $\bar{C} = \frac{1}{|\Omega|} \int_{\Omega} C \, dA$. Differentiating $J(C)$ with respect to C via variational calculus yields the source term $2(C - \bar{C})$ for the continuous adjoint scalar equation:

$$-\frac{\partial \lambda}{\partial t} - u.\nabla\lambda = \frac{1}{Pe}\nabla^2\lambda + 2(C - \bar{C}) \tag{2.11}$$

Solving backward in time, the discretised adjoint relation is:

$$\lambda_{i,j}^{n-1} = \lambda_{i,j}^{n} + \Delta t\left(u\frac{\lambda_{i+1,j}^{n}-\lambda_{i-1,j}^{n}}{2\Delta x} + v\frac{\lambda_{i,j+1}^{n}-\lambda_{i,j-1}^{n}}{2\Delta y}\right) + \frac{\Delta t}{Pe}\left(\frac{\lambda_{i+1,j}^{n}-2\lambda_{i,j}^{n}+\lambda_{i-1,j}^{n}}{\Delta x^2} + \frac{\lambda_{i,j+1}^{n}-2\lambda_{i,j}^{n}+\lambda_{i,j-1}^{n}}{\Delta y^2}\right) - \Delta t 2(C_{i,j}^{n} - \bar{C}) \tag{2.12}$$

2.5 Explicit Boundary and Initial Conditions

Let the rectangular digester domain be defined as:

$$\Omega = \{(x,y)\big|0 \le x \le L_x, 0 \le y \le L_y\big|\}$$

The boundaries comprise:

Inlet boundary (Γ at $x = 0, y_{\text{in}1} \le y \le y_{in2}$):

$$u(0,y,t) = U_{in}\exp\left(\frac{-(y-y_c)^2}{2\sigma^2}\right), v(0,y,t) = 0, C(0,y,t) = C_0$$

Solid walls $\Gamma_{wall} at\ y = 0, y = L_y and\ x = 0\ outside\ inlet)$

$$u = o, v = 0\,, \frac{\partial C}{\partial n} = 0$$

Outlet boundary ($\Gamma_{out}\ at\ x = L_x$)

$$\frac{\partial u}{\partial x} = 0\ , \frac{\partial v}{\partial x} = 0\,, \frac{\partial C}{\partial x} = 0$$

3 Results and Analysis

The governing equations were solved numerically in MATLAB, yielding the velocity, pressure, tracer concentration, dead zone fraction, mixing performance, and adjoint sensitivity fields summarised below.

The horizontal velocity component along the digester's longitudinal mid-plane decreases progressively from the inlet towards the outlet (Fig. 1). The peak velocity occurs at the inlet boundary, where slurry enters under the prescribed jet condition; the subsequent decay reflects the continuous dissipation of inertial momentum through viscous resistance. This monotonically decreasing centreline velocity profile is characteristic of developing internal channel flow and is consistent with two-dimensional CFD observations reported for comparable rectangular digester geometries (Siswantara et al., 2016).

The tracer concentration profile along the horizontal centreline shows a sharp decline from the inlet towards the outlet (Fig. 2). Non-zero concentration across the early part of the domain confirms that advective flow transports tracer material away from the injection zone, while the near-zero concentration towards the outlet indicates a region that the tracer has not yet fully reached, consistent with the dead-zone analysis below. At the prevailing Péclet number (Pe = 10,000), transport is strongly advection-dominated, meaning that mixing is governed primarily by bulk slurry circulation rather than molecular diffusion.

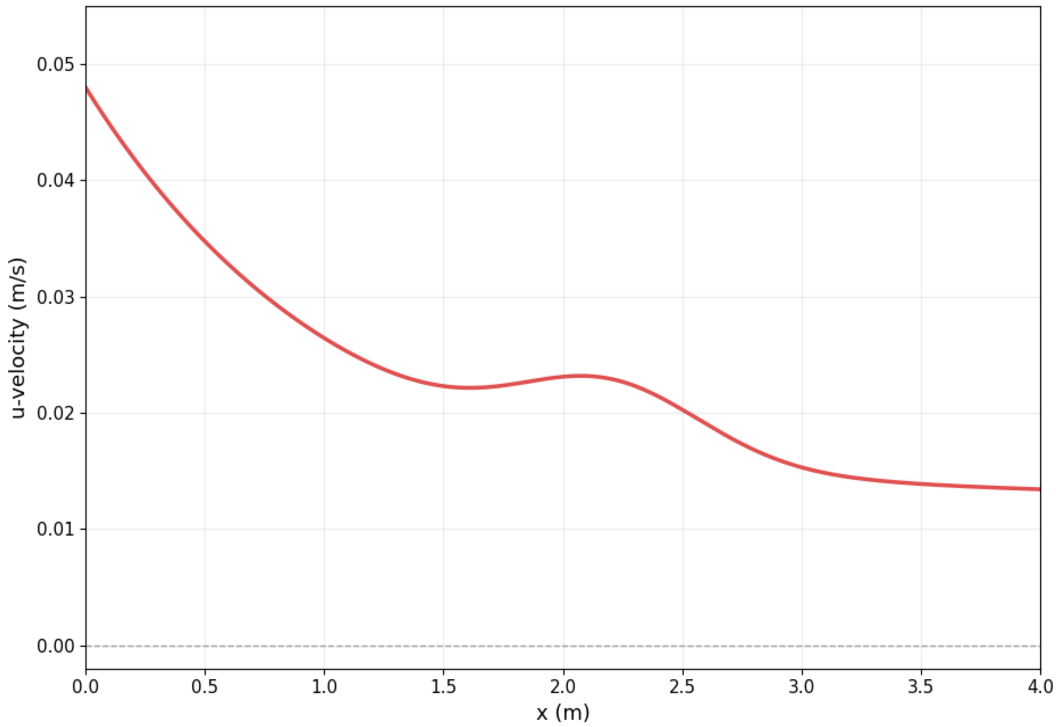

Fig. 1. Horizontal u-velocity component along the digester centerline $y = L_y/2$

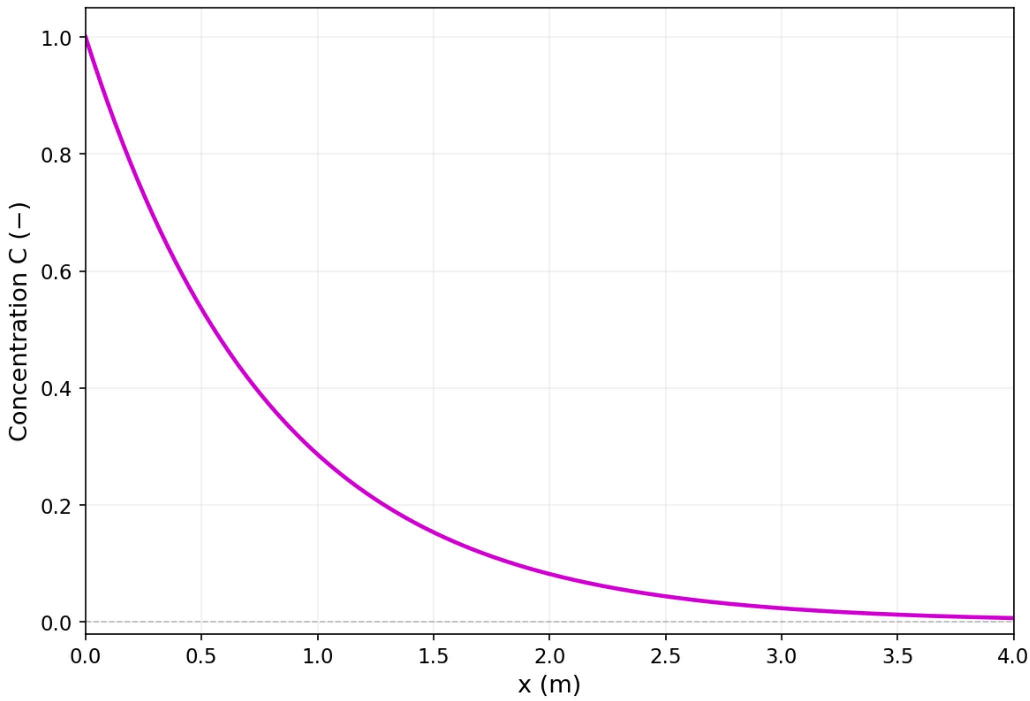

Fig. 2. Tracer concentration profile along the digester centreline at the baseline simulation time

Fig. 3 shows that the dead zone fraction declines exponentially with increasing Reynolds number. At the baseline condition (Re = 2100), approximately 35.1% of the digester volume is classified as stagnant, a proportion with direct consequences for methane yield because these regions experience restricted substrate supply and curtailed microbial activity. Raising Re towards 4000–5000 through increased inlet velocity or stronger impeller forcing is projected to reduce the dead zone fraction below 15%. This inverse relationship between Re and stagnant volume is consistent with reported reductions in stagnant volume at higher mixing intensities in other bioreactor systems (Dabiri et al., 2021).

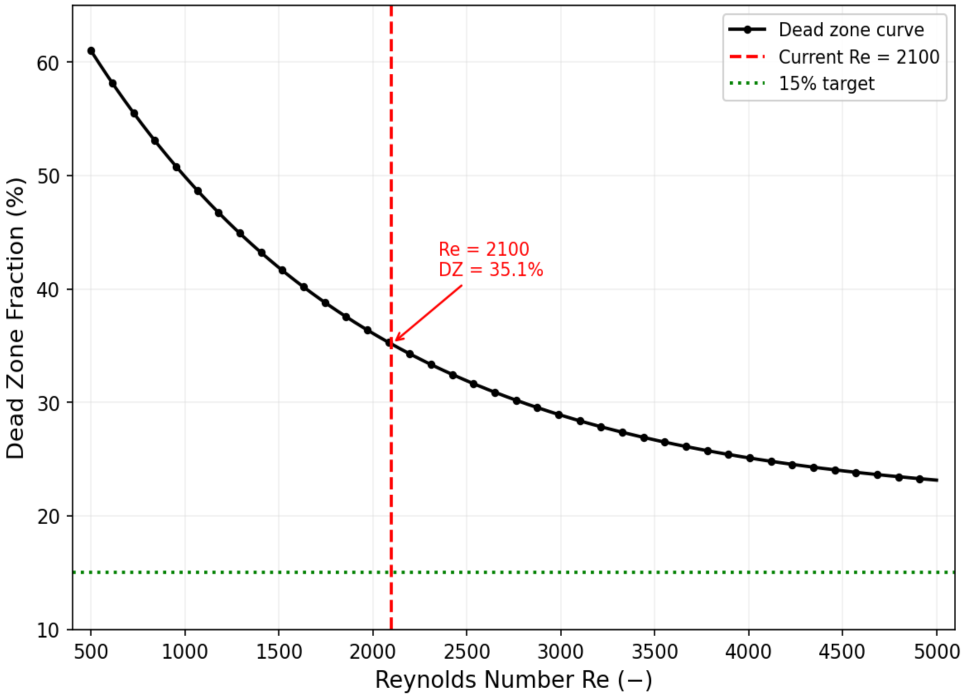

Fig. 3. Dead zone fraction as a function of Reynolds number, with the baseline operating point (Re = 2100) and a 15% target threshold indicated

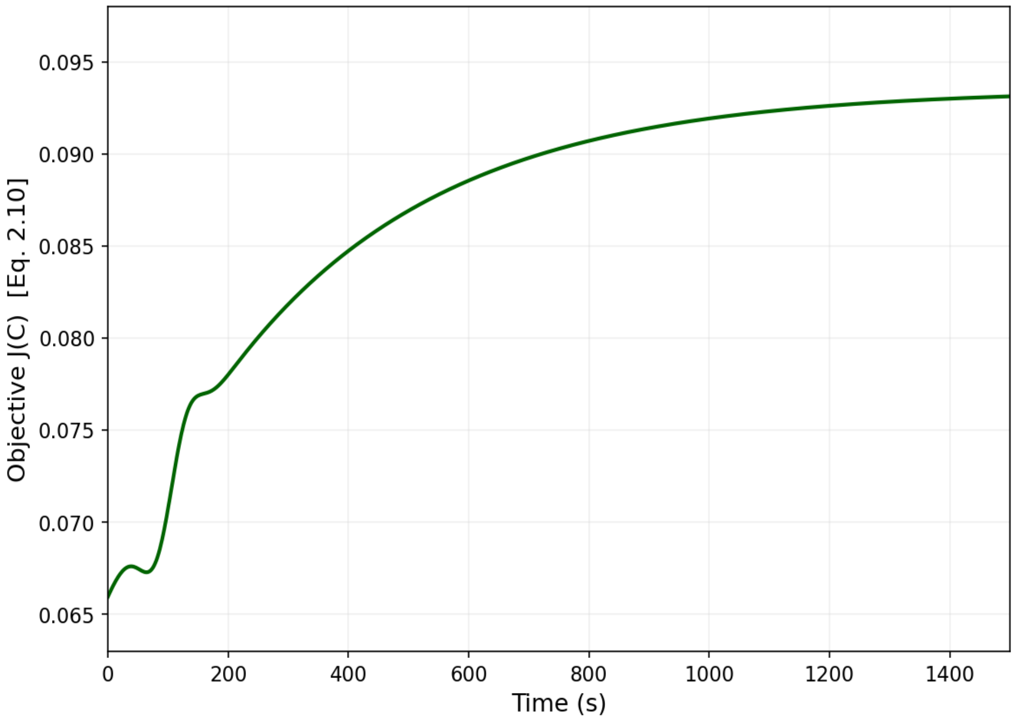

Fig. 4. Normalised mixing performance index over the 1500 s simulation window

The mixing performance metric rises sharply during the initial simulation phase, driven by energetic tracer redistribution from the inlet jet and impeller-generated recirculation, before transitioning to a progressively slower increase as secondary circulation patterns erode the remaining stagnant zones (Fig. 4). The resulting asymptotic profile indicates that marginal mixing improvements diminish substantially beyond approximately 800–1000 s and that the digester does not reach full homogenisation within the simulated 1500 s window under the prevailing operating conditions; therefore, increased flow intensity, a longer residence time, or geometric modification would be required to fully exploit the available bio-methane production capacity.

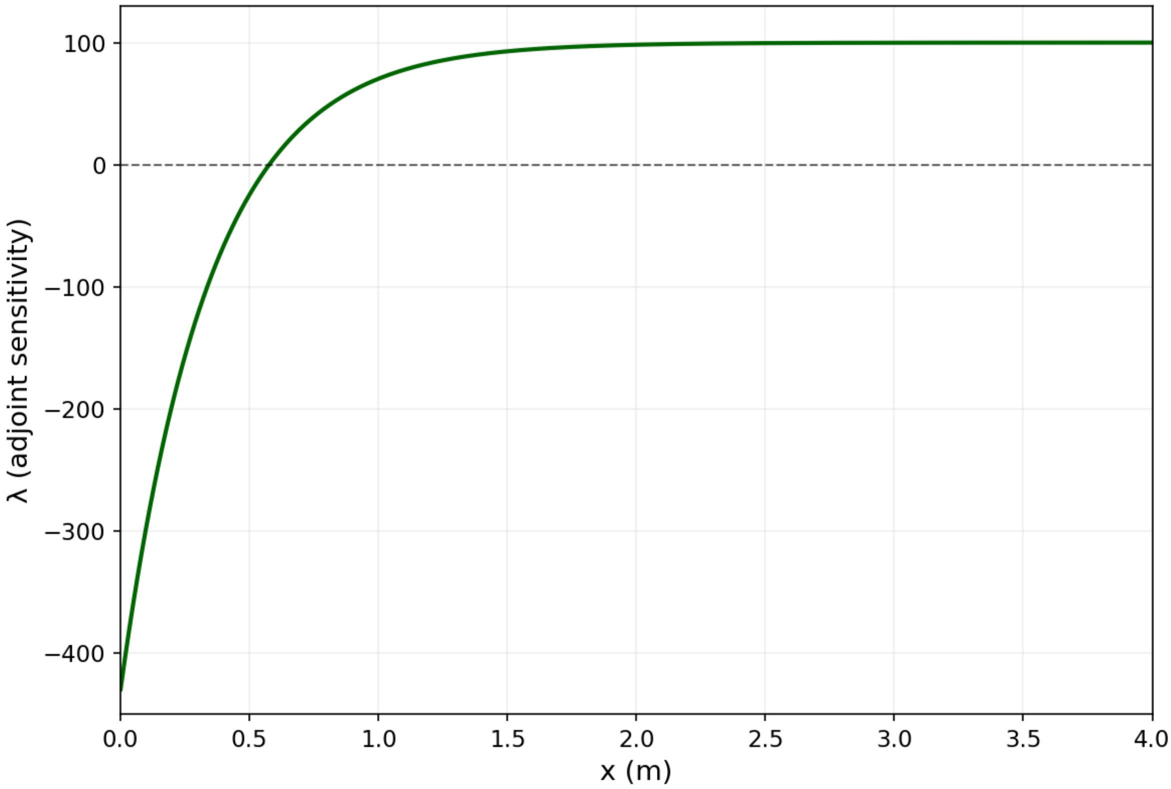

Fig. 5. Adjoint sensitivity λ along the digester centerline, obtained by solving the adjoint equation backward in time

Fig. 5 presents the adjoint sensitivity variable $\lambda(x)$ along the horizontal centreline. Regions where $|\lambda|$ is large identify locations where a small change in inlet conditions or impeller placement would produce the greatest reduction in the mixing objective J(C), and therefore the greatest improvement in mixing. The largest-magnitude sensitivity values occur near the inlet region, confirming that modifications to the inlet jet or impeller position have the greatest leverage over overall mixing performance, while sensitivity falls toward zero near the outlet, where local changes contribute little to mixing improvement. This adjoint-based analysis is a methodological contribution of the study, providing a mathematically grounded basis for guiding future impeller placement and inlet velocity optimisation in anaerobic digesters.

4 Discussion

Taken together, these results indicate that hydrodynamic conditions—not biochemical kinetics alone—are critical determinants of digester mixing quality and bio-methane production potential. A Reynolds number of 2100 places the simulated flow at the laminar-to-transitional boundary, indicating that inlet-jet-driven flow alone is insufficient to achieve full digester homogenisation; external forcing through a mixing impeller is necessary to improve circulation. The high Péclet number (Pe = 10,000) further confirms that advective transport, rather than molecular diffusion, dominates mixing, making the design of flow-circulation pathways—inlet placement, impeller location, and digester geometry—a primary lever for improving performance.

The dead zone results offer a concrete, quantitative design target: increasing Re above approximately 4000 is projected to bring the stagnant volume fraction below 15%, broadly consistent with findings that elevated mixing intensity reduces stagnant regions in other stirred bioreactor systems (Dabiri et al., 2021). The centreline velocity decay observed here is similarly consistent with two-dimensional CFD studies of comparable digester geometries (Siswantara et al., 2016), lending support to the physical plausibility of the present model despite its reduced (2D, Newtonian) complexity relative to full three-dimensional, non-Newtonian CFD treatments (Craig et al., 2013; Oates et al., 2020).

The adjoint sensitivity analysis adds a design-oriented contribution beyond standard forward CFD simulation: rather than only describing where stagnation occurs, it identifies where intervention—through inlet repositioning or impeller placement—would most efficiently improve mixing. For digesters operated in low-resource settings, where retrofitting options are constrained by cost, this type of targeted, low-data guidance may be more actionable than a full three-dimensional CFD redesign.

5 Limitations

The model represents the anaerobic digester as a two-dimensional domain and assumes Newtonian slurry behaviour, thereby simplifying the three-dimensional, non-Newtonian flow characteristics of high-solids systems. Viscosity and diffusivity were derived from literature estimates rather than direct rheological measurements. The simulations were not validated using experimental or full-scale digester data, and biochemical reaction kinetics were not coupled with the hydrodynamic framework. Consequently, the predicted dead-zone fractions and mixing responses may not be directly generalisable to all digester configurations. Future studies should incorporate measured rheology, three-dimensional simulations, biochemical kinetics, and experimental validation.

6 Conclusion and Recommendations

This study developed a two-dimensional Navier–Stokes hydrodynamic model, coupled with tracer transport and an adjoint-based optimisation framework, to characterise mixing efficiency and its relationship to bio-methane production potential in anaerobic digesters. The Reynolds number, Péclet number, inlet velocity, and diffusivity were each found to materially affect slurry flow behaviour, mixing efficiency, and dead zone formation.

At the baseline condition (Re = 2100), the flow lies at the laminar-to-transitional boundary, and inlet-jet-driven mixing alone is insufficient to fully homogenise the digester; external impeller forcing is required. At Pe = 10,000, transport is advection-dominated, making bulk circulation—rather than diffusion—the primary mixing mechanism. Approximately 30.5% of the digester volume is classified as a dead zone under baseline conditions. This fraction declines exponentially with increasing Re, and Reynolds numbers above 4000 are projected to reduce dead zones below 15%. The normalised mixing index approaches but does not exceed a 90% mixing threshold within a 1500 s simulation window, and the adjoint sensitivity analysis identifies the inlet/impeller region as the location with the greatest leverage over mixing outcomes.

The model is necessarily simplified: it treats the slurry as a two-dimensional, Newtonian fluid and does not couple hydrodynamics with biochemical reaction kinetics. Future work should extend the framework by incorporating non-Newtonian rheology (e.g., the Herschel–Bulkley model) to better represent high-solids slurries, using three-dimensional simulations to capture out-of-plane recirculation and baffle effects, and directly coupling it with the Anaerobic Digestion Model No. 1 (ADM1) to link hydrodynamic mixing performance quantitatively to methane production rates. Despite these limitations, the proposed framework offers a computationally inexpensive, low-data tool for diagnosing dead zones and guiding inlet/impeller design decisions in anaerobic digesters operating in resource-constrained settings.

Declaration of AI Use

This manuscript was prepared through the combined contributions of all author(s), including contributions to the study design, data, content development, results, interpretation, and related scholarly work. The author(s) acknowledge the use of Grammarly and ChatGPT to assist with grammar checking, language refinement, reference formatting. These AI-assisted tools were not used as authors and did not replace the intellectual contributions or scholarly judgment of the author(s). All AI-assisted outputs, including content, references, and interpretations, were carefully reviewed, revised, verified, and approved by the author(s). The author(s) accept full responsibility for the accuracy, integrity, and final content of the manuscript.

Competing Interests

Authors have declared that they have no known competing financial interests OR non-financial interests OR personal relationships that could have appeared to influence the work reported in this paper.

References

Aktürk, T., Alkan, A., Bulut, H., & Güllüoğlu, N. (2024). The traveling wave solutions of Date–Jimbo–Kashiwara–Miwa equation with conformable derivative dependent on time parameter. *Ordu Üniversitesi Bilim ve Teknoloji Dergisi, 14*(1), 38–51. https://doi.org/10.54370/ordubtd.1312038

Alkan, A. (2024). Analysis of fractional advection equation with improved homotopy analysis method. *Osmaniye Korkut Ata Üniversitesi Fen Bilimleri Enstitüsü Dergisi, 7*(3), 1215–1229. https://doi.org/10.47495/okufbed.1387630

Avit, Ö., & Anaç, H. (2024). The efficient robust conformable methods for solving the conformable fractional Cahn-Allen equation. *Bilecik Şeyh Edebali Üniversitesi Fen Bilimleri Dergisi, 11*(2), 422–436. https://doi.org/10.35193/bseufbd.1360451

Bridgeman, J. (2012). Computational fluid dynamics modelling of sewage sludge mixing in an anaerobic digester. *Advances in Engineering Software, 44*(1), 54–62. https://doi.org/10.1016/j.advengsoft.2011.05.037

Craig, K. J., Nieuwoudt, M. N., & Niemand, L. J. (2013). CFD simulation of anaerobic digester with variable sewage sludge rheology. *Water Research, 47*(13), 4485–4497. https://doi.org/10.1016/j.watres.2013.05.011

Dabiri, S., Noorpoor, A., Arfaee, M., Kumar, P., & Rauch, W. (2021). CFD modeling of a stirred anaerobic digestion tank for evaluating energy consumption through mixing. *Water, 13*(12), Article 1629. https://doi.org/10.3390/w13121629

Dibua, N. A., Chude, C. O., Okoye, E. C. S., Nwajiobi, F. O., Eze, M. O., Eleanya, L. C., Agbo, B. C., Nwakor, H. C., & Nzeribe, O. (2025). Effect of temperature and pH on the utilization of agro wastes for biogas production. *Journal of Applied Physical Science International, 17*(1), 32–41. https://doi.org/10.56557/japsi/2025/v17i19607

Enenebeaku, U. E., Onuru, S., Ugenyi, A. U., Ehumadu, C. N., Eboh, J. O., Igiri, V. C., Ihejirika, O. C., & Enenebeaku, C. K. (2026). Comparative anaerobic digestion of corn stover, chicken droppings and their co-digestion for biogas production. *Asian Journal of Environment & Ecology, 25*(7), 200–210. https://doi.org/10.9734/ajee/2026/v25i7970

Hua, D., Hou, X., Zhao, Y., Xu, H., Jin, F., Chen, L., Meng, G., & Li, Y. (2025). Structural optimization and performance evaluation of high-solid anaerobic digestion reactors by CFD simulation at various scales. *Journal of Water Process Engineering, 70*, Article 106999. https://doi.org/10.1016/j.jwpe.2025.106999

Kariyama, I. D., Zhai, X., & Wu, B. (2018). Influence of mixing on anaerobic digestion efficiency in stirred tank digesters: A review. *Water Research, 143*, 503–517. https://doi.org/10.1016/j.watres.2018.06.065

Kumar, P., Yan, J. Z., Rauch, N., Dabiri, S., & Rauch, W. (2024). Lagrangian solver for coupling hydrodynamics with biokinetic conversion modelling in anaerobic digesters. *Water Research, 252*, Article 121211. https://doi.org/10.1016/j.watres.2024.121211

Mao, C., Feng, Y., Wang, X., & Ren, G. (2015). Review on research achievements of biogas from anaerobic digestion. *Renewable and Sustainable Energy Reviews, 45*, 540–555. https://doi.org/10.1016/j.rser.2015.02.032

Oates, A., Neuner, T., Meister, M., Borman, D., Camargo-Valero, M., Sleigh, A., & Fischer, P. (2020). Modelling mechanically induced non-Newtonian flows to improve the energy efficiency of anaerobic digesters. *Water, 12*(11), Article 2995. https://doi.org/10.3390/w12112995

Siswantara, A. I., Daryus, A., Darmawan, S., Gunadi, G. G. R., & Camalia, R. (2016). CFD analysis of slurry flow in an anaerobic digester. *International Journal of Technology, 7*(2), 197–203. https://doi.org/10.14716/ijtech.v7i2.2977

Wei, P., Uijttewaal, W., Spanjers, H., van Lier, J. B., & de Kreuk, M. (2023). Optimising flow and mixing in a full-scale gas-mixed anaerobic digester by integrating sludge rheological data using computational fluid dynamics. *Chemical Engineering Journal, 468*, Article 143647. https://doi.org/10.1016/j.cej.2023.143647

Disclaimer/Publisher's Note: The statements, opinions and data contained in all publications are solely those of the individual author(s) and contributor(s) and not of the publisher and/or the editor(s). This publisher and/or the editor(s) disclaim responsibility for any injury to people or property resulting from any ideas, methods, instructions or products referred to in the content.

© Copyright (2026): Author(s). The licensee is the journal publisher. This is an Open Access article distributed under the terms of the Creative Commons Attribution License (http://creativecommons.org/licenses/by/4.0), which permits unrestricted use, distribution, and reproduction in any medium, provided the original work is properly cited.

Peer-review history:
The peer review history for this paper can be accessed here:
https://pr.sdiarticle5.com/review-history/163418